## A

Fig. 4. (A) 3C analysis examining interaction of the *Admp* enhancer with nearby regions. A schematic representation of the genomic organization of *Pinhead* and *Admp* and restriction fragments used is shown below the graph. Blue and yellow triangles indicate the SBEs and E boxes in the P and A enhancers. The brown box indicates the G enhancer. The graph shows interactions of fragment 5 with the other fragments. The *y* axis indicates normalized interaction frequency calculated as fold difference relative to the control reaction using bacterial artificial chromosome DNA. Blue bars indicate embryos with Bmp2/4 overexpression, which leads to up-regulation of *Pinhead* transcription. Yellow bars indicate embryos with noggin overexpression, which leads to down-regulation of *Pinhead* transcription. Error bars indicate standard errors of quantitative real-time fluorescence polymerase chain reaction. **(B)** Models of chromosome conformations of the P (blue), A (yellow), and G (brown) enhancers when *Pinhead* transcription is active (left) and inactive (right).
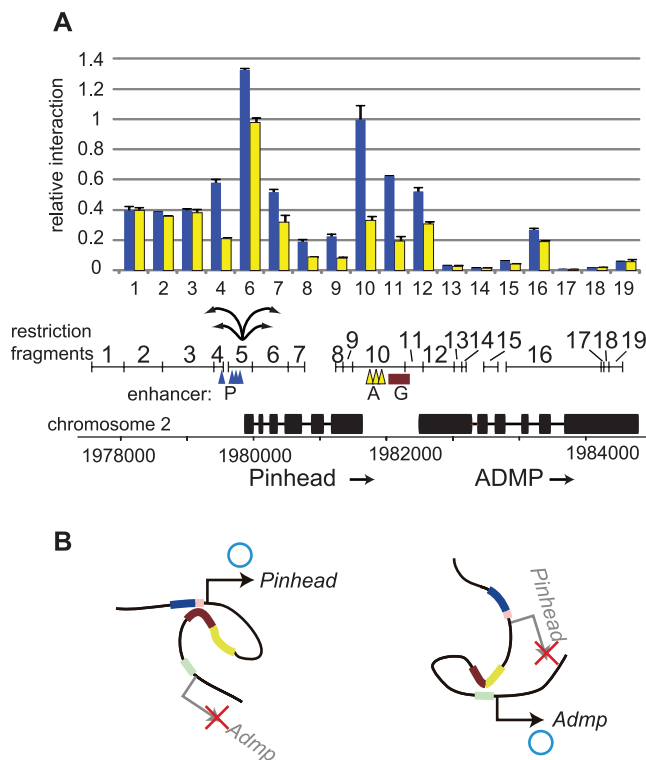
indicate that Pinhead plays a key role in this system (fig. S11). Because Pinhead specifically interacts with Admp, Pinhead antagonizes Admp activity after Admp induces *Pinhead* transcription, preventing Admp activity from propagating further laterally and dorsally, but does not affect Bmp2/4 signaling. Furthermore, *Pinhead* transcription suppresses *Admp* transcription, thereby ensuring their mutually exclusive expression. This occurs mainly through competition for the G enhancer, a competition that *Pinhead* always wins when the *Admp/BMP* signal is active. Because the genomic configuration of *Pinhead* and *Admp* is widely conserved from arthropods to vertebrates, this dual negative regulation may be conserved as well.

References and Notes

1. R. Dosch, C. Niehrs, *Mech. Dev.* **90**, 195 (2000).
2. B. Reversade, E. M. De Robertis, *Cell* **123**, 1147 (2005).
3. K. Joubin, C. D. Stern, *Cell* **98**, 559 (1999).
4. Z. Lele, M. Nowak, M. Hammerschmidt, *Dev. Dyn.* **222**, 681 (2001).
5. V. Willot *et al.*, *Dev. Biol.* **241**, 59 (2002).
6. T. Dickmeis *et al.*, *Dev. Genes Evol.* **211**, 568 (2001).
7. M. A. Gaviño, P. W. Reddien, *Curr. Biol.* **21**, 294 (2011).
8. P. Lemaire, W. C. Smith, H. Nishida, *Curr. Biol.* **18**, R620 (2008).
9. K. S. Imai, M. Levine, N. Satoh, Y. Satou, *Science* **312**, 1183 (2006).
10. A. Pasini *et al.*, *PLoS Biol.* **4**, e225 (2006).
11. K. S. Imai, K. Hino, K. Yagi, N. Satoh, Y. Satou, *Development* **131**, 4047 (2004).
12. S. Kenwrick, E. Amaya, N. Papalopulu, *Dev. Dyn.* **229**, 289 (2004).
13. Y. Satou, S. Wada, Y. Sasakura, N. Satoh, *Dev. Genes Evol.* **218**, 715 (2008).
14. J. Dekker, K. Rippe, M. Dekker, N. Kleckner, *Science* **295**, 1306 (2002).

Landscape of Somatic Retrotransposition in Human Cancers

Eunjung Lee,[1,2] Rebecca Iskow,[3] Lixing Yang,[1] Omer Gokcumen,[3] Psalm Haseley,[1,2] Lovelace J. Luquette III,[1] Jens G. Lohr,[4,5] Christopher C. Harris,[6] Li Ding,[6] Richard K. Wilson,[6] David A. Wheeler,[7] Richard A. Gibbs,[7] Raju Kucherlapati,[2,8] Charles Lee,[3] Peter V. Kharchenko,[1,9]* Peter J. Park,[1,2,9]* and The Cancer Genome Atlas Research Network

Transposable elements (TEs) are abundant in the human genome, and some are capable of generating new insertions through RNA intermediates. In cancer, the disruption of cellular mechanisms that normally suppress TE activity may facilitate mutagenic retrotranspositions. We performed single-nucleotide resolution analysis of TE insertions in 43 high-coverage whole-genome sequencing data sets from five cancer types. We identified 194 high-confidence somatic TE insertions, as well as thousands of polymorphic TE insertions in matched normal genomes. Somatic insertions were present in epithelial tumors but not in blood or brain cancers. Somatic L1 insertions tend to occur in genes that are commonly mutated in cancer, disrupt the expression of the target genes, and are biased toward regions of cancer-specific DNA hypomethylation, highlighting their potential impact in tumorigenesis.

Transposable elements (TEs) have proliferated in mammalian genomes by integrating new copies primarily through RNA-mediated mechanisms. Whereas most TEs are inactive remnants fixed within the human population, younger TEs account for much of the structural variation among individual genomes (*1*). TE activity in somatic tissues is normally repressed through epigenetic and post-transcriptional mechanisms (*2–4*), but some TEs escape repression and generate new polymorphic insertions during the transient release of these repression mechanisms in germ cells and during early embryonic development (*5–7*). Some of these insertions can occur later in life (*8*) and result in disease-causing gene alterations (*9*), such as the few examples reported in colon and lung

[1]Center for Biomedical Informatics, Harvard Medical School, Boston, MA 02115, USA. [2]Division of Genetics, Brigham and Women's Hospital, Boston, MA 02115, USA. [3]Department of Pathology, Brigham and Women's Hospital, and Harvard Medical School, Boston, MA 02115, USA. [4]The Eli and Edythe Broad Institute, Cambridge, MA 02412, USA. [5]Dana-Farber Cancer Institute, Boston, MA 02115, USA. [6]The Genome Institute, Washington University, School of Medicine, St. Louis, MO 63108, USA. [7]Human Genome Sequencing Center, Baylor College of Medicine, Houston, TX 77030, USA. [8]Department of Genetics, Harvard Medical School, Boston, MA 02115, USA. [9]Informatics Program, Children's Hospital, Boston, MA 02115, USA.

*To whom correspondence should be addressed. E-mail: peter_park@harvard.edu (P.J.P.); peter.kharchenko@post.harvard.edu (P.V.K.)

cancers (*10*, *11*). However, despite its mutagenic potential, the extent to which somatic retrotransposition contributes to tumorigenesis in various tissues remains largely unexplored. Here, we identify TE integration sites at single-nucleotide resolution, characterizing the insertional mechanisms and distinguishing retrotransposition from other types of genomic rearrangements common in cancer genomes.

Analysis of TEs with short-read sequencing is challenging, because numerous, often nearly identical TE instances make it difficult to discern the true source of the sequenced fragments. Detection of somatic TE insertions in cancer genomes is further complicated by heterozygosity, cellular and genetic heterogeneity of tumor samples, and complex genomic rearrangements found in many cancers. We developed Tea (TE analyzer), a computational method that detects the exact position and mechanism of TE insertions from paired-end whole-genome sequencing data with high accuracy (Fig. 1).

We applied Tea to whole-genome sequencing data from tumor and matched normal blood samples from a total of 43 colorectal, prostate, ovarian, multiple myeloma, and glioblastoma cancer patients (table S1). Our analysis revealed 194 high-confidence somatic TE insertions (183 L1s,

10 Alus, and 1 ERV) with the average per tumor type ranging from 0 to 29 (Fig. 2A and table S2). All of the somatic L1 and Alu insertions were observed in the cancers of epithelial cell origin (colorectal, prostate, and ovarian), with colorectal tumors showing the highest frequency of somatic L1 insertions, but not in the blood or brain cancers. Some of the TE insertions detected by our method may be generated by mechanisms other than classical retrotransposition. Although none of the ERV1 family elements are thought to be active in humans, we observed an ERV somatic insertion (PABL_A repeat, ERV1 family) in a myeloma sample in the intron of *DAPK1* (death-associated protein kinase 1), later validated by polymerase chain reaction (PCR) and Sanger sequencing (fig. S1 and tables S3 and S4). Given the small insertion size [375 base pairs (bp)] and 2-bp microhomology at both breakpoint junctions, the ERV1 insertion was likely generated via the microhomology-mediated break-induced repair mechanism (*12*).

One colorectal tumor (CR3518) showed a high somatic TE insertion frequency (106 events) along with microsatellite instability, a high nonsilent single-nucleotide or short insertion/deletion (indel) mutation rate (430 mutations), altered DNA repair pathways via *MLH1* epigenetic silencing and a *POLE* mis-

sense mutation and belonged to the high CpG island methylator phenotype (CIMP-high) (table S5). In contrast, the other colorectal tumors (*13*) were microsatellite-stable, had a low simple mutation rate (45 to 60 mutations), lacked detectable aberrations among the DNA mismatch repair genes tested, and belonged to CIMP-low or non-CIMP methylation subgroups (table S5). Taken together, this suggests the presence of tumor subtypes with respect to TE activity.

A representative set of predicted insertions was selected for PCR-based validation (supplementary text S1). We confirmed 25 out of 26 somatic L1 insertions examined in colorectal tumors and all of the 13 L1 insertions examined in ovarian cancers, resulting in an overall accuracy of 97% (table S3). Six junctions and two entire L1 insertions were further examined by using Sanger sequencing, confirming the presence of the L1 sequences, insertion breakpoints, target-site duplication (TSD) sequences, and poly-A tails (table S4). The sensitivity of detection depends on the purity of the tumor samples and clonality of the events. Our approach was able to detect heterozygous insertions in samples with tumor purity as low as 49% (fig. S2). Events present at lower frequency, such as insertions accumulated at later stages of tumorigenesis, were likely missed. Our
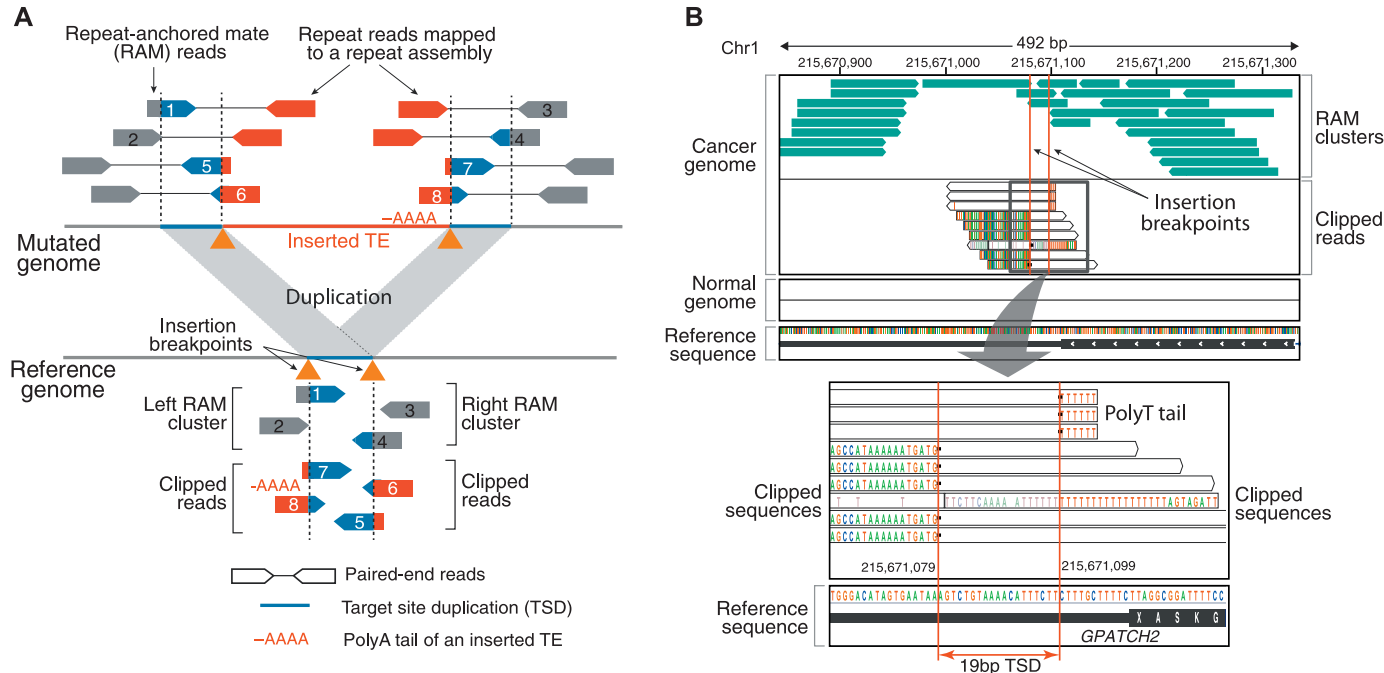
Fig. 1. (**A**) To detect somatic insertions of TEs, paired-end sequencing data from tumor and matched normal samples are aligned to both the reference genome and a custom repeat assembly of canonical and divergent TE sequences. Two types of supporting reads are identified: (i) repeat-anchored mate (RAM) reads, in which one of the paired-end reads is mapped to a unique location in the genome, whereas the other is associated with a TE (reads 1 to 4), and (ii) clipped reads, which span the TE insertion breakpoints and show partial alignment to the reference or the repeat assembly (reads 5 to 8). The distances between the clipping positions and the clipped sequences are used to infer the insertion mechanism. For instance, duplicated sequences at the insertion site (TSD) and the poly-A tail of the inserted TE are characteristics of an endonuclease-mediated target-primed retrotransposition. (**B**) Example: a validated somatic L1 insertion in the 3′ UTR of *GPATCH2* in colorectal cancer (CR3518). The top chart displays two clusters of RAM reads (green) whose mate pairs (not shown) are associated with L1 repeat sequences. Clipped (partially aligned) reads spanning the insertion breakpoint are shown underneath, with each nucleotide in a different color (nucleotides matching the reference are not shown). The consecutive red bases to the right of the insertion come from the poly-T tail of the inserted L1 in the negative orientation. The separation of clipped read positions between the strands reveals a 19-bp TSD (bottom). No RAMs or clipped reads are observed in the matched normal (blood) sample.

approach cannot detect insertions landing in highly repetitive regions, so the true number of events is likely to be higher.

Of the 194 detected somatic TE insertions, 64 were located within 62 annotated genes (table S2), including those implicated for tumor suppressor functions through deletions or epigenetic silencing (supplementary text S2): for example, *NELL1*, *DBC1*, *ROBO2*, and *PARK2* (14–18). The affected set was enriched for genes associated with cell-adhesion functions ($P = 9.8 \times 10^{-5}$; false discovery rate = 0.04), including *CDH12*, *ROBO2*, *NRXN3*, *FPR2*, *COL11A1*, *NEGR1*, *NTM*, and *CTNNA2*. We examined nucleotide mutation frequencies (single nucleotide or small indel) across 232 additional colorectal tumors and found that the TE target genes are significantly enriched for frequently mutated genes (Fig. 2B, bootstrap Kolmogorov-Smirnov test, $P < 10^{-15}$ for both nonsilent and all mutations). A separate

analysis of 40 genes targeted by the somatic TE insertions only in colorectal tumors also showed significant enrichment of frequently mutated genes ($P < 10^{-15}$; fig. S3). Because recurrently mutated genes are likely to be important drivers of tumorigenesis, our results suggest potential contribution of TE insertions to cancer development (19, 20).

Although none of the somatic events hit coding regions, insertions of TE sequence in untranslated regions (UTRs) or intronic regions can disrupt gene expression (21). Indeed, over a quarter of the identified disease-causing TE insertions are located in introns or UTRs (9). We thus compared the mRNA levels of the 45 genes hit by somatic TEs in colorectal cancer between the affected tumor and normal samples. We found that expression of the targeted genes is typically altered in the sample carrying the TE insertion, resulting in significantly lower expression levels on average ($P = 6.3 \times 10^{-4}$; Fig. 2C and fig. S4). The

impact of L1 insertions may depend on the orientation of the L1 insertion relative to the target gene, with antisense insertions being less disruptive (21). Indeed, expression of the 27 genes targeted by sense insertions showed significant decrease ($P = 3.9 \times 10^{-4}$), whereas expression reduction of the 18 genes targeted in the antisense direction did not reach statistical significance ($P = 0.17$). Two somatic L1 insertions were found in the 3′ UTRs of *F13B* and *GPATCH2* in one colorectal tumor (CR3518) (Fig. 1B and fig. S5). The insertion in *GPATCH2*, a gene that has been implicated in breast cancer growth (22), coincided with significant reduction of its expression level ($P = 3.3 \times 10^{-5}$; Fig. 2C and fig. S4).

To contrast the features of somatic TE insertions in cancer genomes with polymorphic insertions in human populations, we analyzed 44 normal genomes (41 normal blood samples from cancer patients and three healthy individuals from the
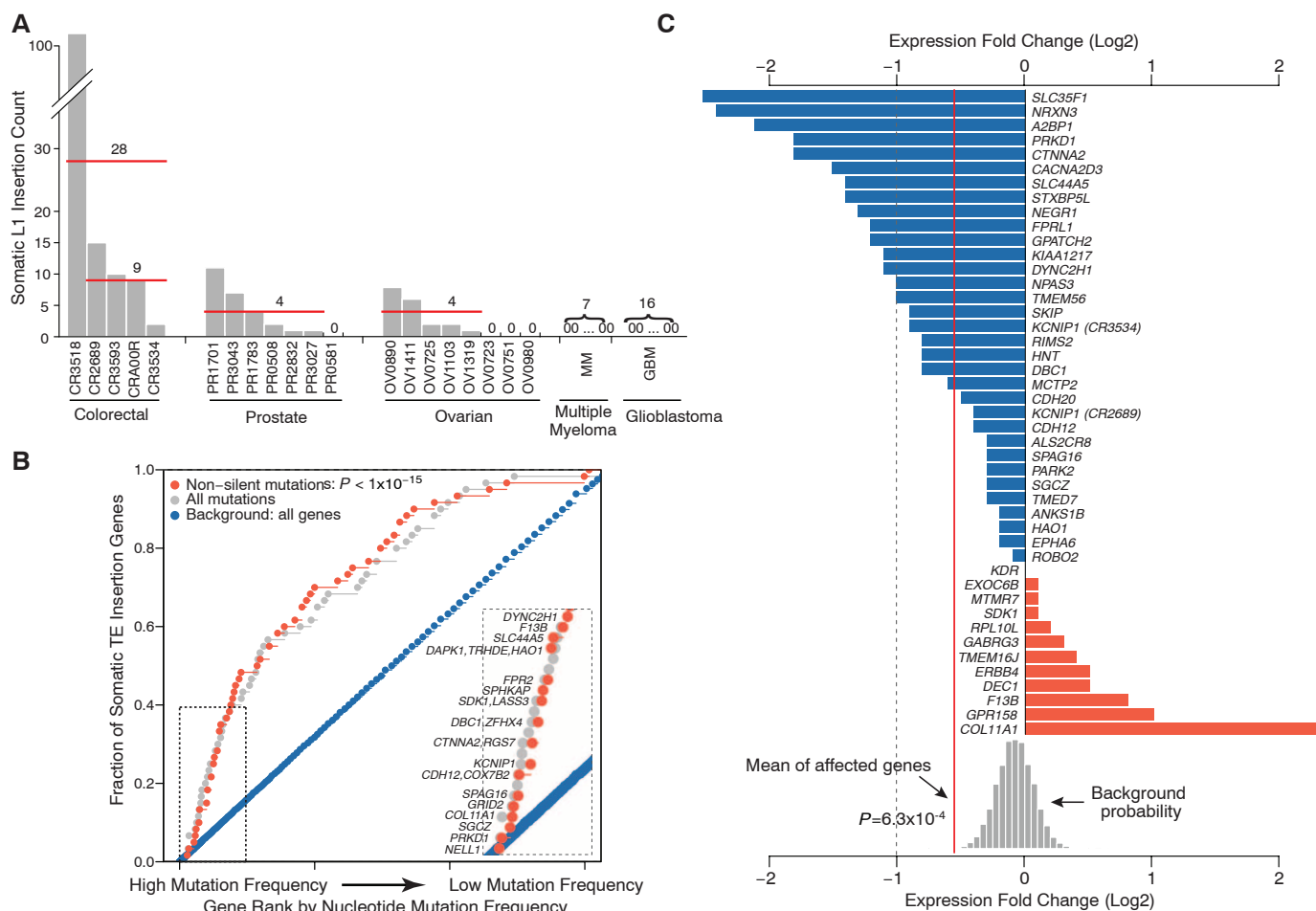

Fig. 2. (**A**) Frequency of high-confidence somatic L1 insertions varies across 5 colorectal, 7 prostate, 8 ovarian, 7 multiple myeloma, and 16 glioblastoma tumors. Three epithelial cancers (colorectal, prostate, and ovarian) show frequent somatic L1 insertions, whereas no insertions are observed in the blood and brain cancers. One colorectal tumor (CR3518) contains 102 L1 insertions, increasing the average somatic event frequency for colorectal tumors from 9 to 28 when this sample is included. (**B**) The genes affected by somatic TE insertions are significantly enriched for genes with high mutation rates as estimated from the exome sequencing data of 228 additional

colorectal tumors ($P < 1 \times 10^{-15}$). The mutation frequency of each gene was adjusted for its total exon size. (Inset) The top 15 genes with nonsilent mutations. (**C**) The transcript levels of 45 genes with somatic TE insertions in colorectal tumors were compared with those from 28 normal colorectal tissues, and the expression fold changes are shown. Overall, the genes with a TE insertion were significantly down-regulated in tumors ($P = 6.3 \times 10^{-4}$, background distribution based on randomly sampled gene sets). *KCNIP1* appears twice because of two somatic insertions in two different samples. The dashed line marks 50% reduction in expression.

HapMap project) and identified a total of 7449 TE insertions (5531 Alus, 1645 L1s, 225 SVAs, 31 ERVKs, and 17 ERVL-MaLRs) that are absent in the reference genome (tables S6 to S8). Because the majority of such polymorphic events are passed down through gametes or generated during early embryonic development, we refer to them as germline insertions. Among the detected germline insertions, 3521 (47%) were polymorphisms not reported in earlier studies (11, 23–27) or the Database of Retrotransposition Insertion Polymorphisms (dbRIP) (28) (fig. S6). Although ERVK family polymorphisms are rare (10 records in dbRIP) and none have been reported for the ERVL-MaLR family, we identified 31 distinct LTR5 and 17 distinct THE1 polymorphic sites (two LTR5 and one THE1 insertions were experimentally validated, supplementary text S1). Each individual genome contained an average of 791 Alu, 169 L1, 33 SVA, and 8 ERV insertions not found in the reference assembly (fig. S6).

On the basis of a partial reconstruction of the inserted L1 sequences (tables S2 and S6), we find that most insertions are not full-length L1 instances but fragments substantially truncated at the 5′ end (Fig. 3A). The trend is more pronounced for somatic insertions, which are truncated more often (Fisher's exact test, $P = 1.3 \times 10^{-12}$), and the truncated sequences are on average significantly shorter (545 versus 1050 bp; Wilcoxon test, $P = 4.1 \times 10^{-7}$). Although most of the somatic L1 insertions originated from young L1Ta subfamilies that are known to be active (table S2 and supplementary text S3), the truncations indicate that the vast majority (>98%) of the somatic insertions would not be competent of further retrotransposition.

The local sequence properties around the identified breakpoints for 64% of the somatic L1 insertions showed both TSDs (≥5 bp) and poly-A tails, which together with the strong 3′ bias of the inserted sequences suggest that the majority of somatic TE insertions in cancers are retrotransposition events driven by the endonuclease-mediated pathway (5). The distribution of TSD lengths showed a peak around 15 bp, characteristic of endonuclease-mediated retrotransposition, for both somatic and germline insertions (Fig. 3B and fig. S6). However, somatic insertions exhibited an additional peak at 0 bp, indicating that some may have been gen-

erated by an alternative mechanism such as the one mediated by DNA breaks that does not result in TSDs (29, 30). Consistent with this, somatic L1 insertions with TSDs show sequence motifs at the breakpoints that correspond to the canonical L1-endonuclease recognition sequence (31), whereas the insertions lacking TSDs do not show such a clear recognition sequence (Fig. 3B).

Somatic and germline L1 insertion sites differ in their genomic distribution and epigenetic characteristics. The germline L1 insertions are significantly depleted from genes (22% depletion, $P = 1.0 \times 10^{-12}$), likely because of strong negative selection acting on such events (32). The somatic L1 insertions do not show such notable depletion (11% depletion, $P = 0.28$) but are nevertheless biased away from transcriptionally active regions (housekeeping genes and common open chromatin regions, figs. S7 to S9). DNA methylation suppresses both TE RNA expression and integration (33), and genome-wide disruption of DNA methylation has been documented in cancers (34). Examination of whole-genome DNA methylation profiles in colorectal cancer (35) shows that somatic L1 insertion sites are significantly

Fig. 3. (**A**) Most of the identified insertions do not contain a full L1 sequence (6 kbp) but are truncated at the 5′ end. The parts of the L1 sequence found within the identified somatic and germline insertions are illustrated as a coverage plot. (**B**) A positive distance between the clipping positions of clipped reads with negative- and positive-strand mapping (Fig. 1B) corresponds to the length of the duplicated sequence at a TSD, whereas a negative or zero

distance corresponds to a microdeletion or lack of duplication at the insertion site. The major TSD peak at ~15 bp is characteristic of an endonuclease-dependent L1 retrotransposition. Sequence analysis around the insertion breakpoints revealed the 5′-TTTT/A-3′ (where the slash in-dicates the insertion breakpoint) motif, consistent with a canonical sequence for L1-endonuclease target sites (31). The insertions belonging to the minor TSD peak (0 to 2 bp) did not show a significant sequence motif.
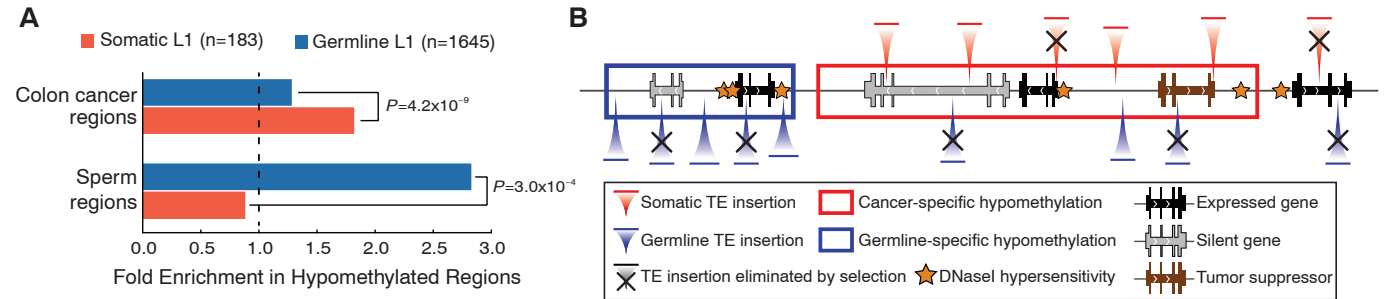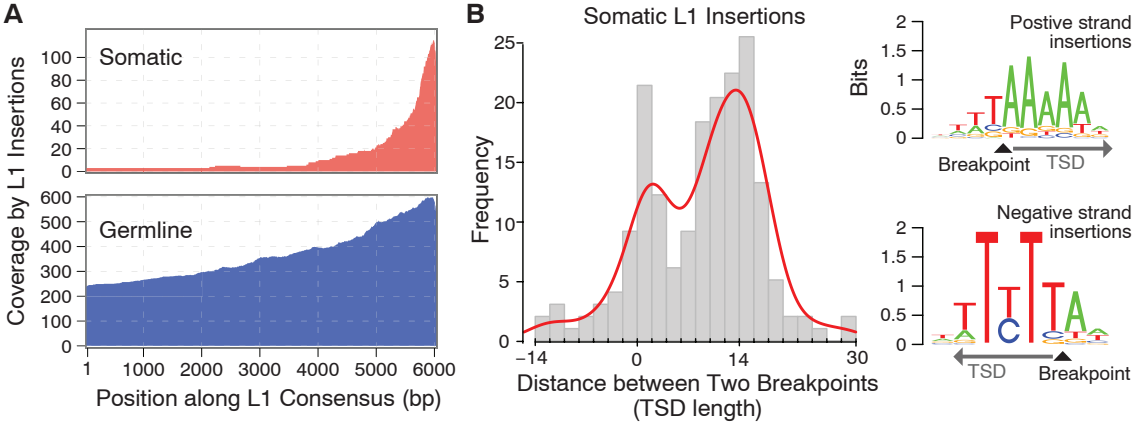

Fig. 4. (**A**) Somatic L1 insertions are biased toward hypomethylated regions in cancer cells. Colon cancer regions were assessed in independent samples. (**B**) A model of TE insertion preferences and subsequent selection process that bias genomic distribution of TE insertions is illustrated. Somatic insertions are strongly biased toward cancer-specific DNA hypomethylation regions (red box) and encounter selection that depletes them from transcriptionally active genes unless such insertions promote tumorigenesis. By contrast, germline insertions are biased toward germline-specific DNA hypomethylation domains (blue box) and are depleted from all genes.

overrepresented within regions of DNA hypomethylation ($P = 4.2 \times 10^{-9}$; Fig. 4A). The L1 insertion bias toward common hypomethylation domains suggests that loss of DNA methylation promotes integration of L1 instances. Supporting this hypothesis, we find that the germline L1 insertions are significantly enriched ($P = 3.0 \times 10^{-4}$) in sperm-specific hypomethylation regions (7), whereas somatic insertions are biased toward cancer-specific hypomethylation regions (Fig. 4).

Our analysis suggests that some TE insertions provide a selective advantage during tumorigenesis, rather than being merely passenger events that precede clonal expansion. We observed differential deregulation of TE activity across and within different cancer types. We also found that such insertions preferentially occur at genes commonly mutated in cancer, including tumor suppressors, substantially disrupting their expression. Although a more extensive panel of matched genomic and epigenetic data is needed to investigate the functional impact of retrotransposition events and the pathways involved, our analysis reveals the extent of TE insertions in human tumors and lays the foundation for determining the role of these events in human neoplasia.

References and Notes

1. J. M. Kidd et al., Cell **143**, 837 (2010).
2. I. A. Maksakova, D. L. Mager, D. Reiss, Cell. Mol. Life Sci. **65**, 3329 (2008).
3. R. K. Slotkin, R. Martienssen, Nat. Rev. Genet. **8**, 272 (2007).
4. N. Yang, H. H. Kazazian Jr., Nat. Struct. Mol. Biol. **13**, 763 (2006).
5. E. T. L. Prak, H. H. Kazazian Jr., Nat. Rev. Genet. **1**, 134 (2000).
6. D. Bourc'his, T. H. Bestor, Nature **431**, 96 (2004).
7. A. Molaro et al., Cell **146**, 1029 (2011).
8. J. K. Baillie et al., Nature **479**, 534 (2011).
9. D. C. Hancks, H. H. Kazazian Jr., Curr. Opin. Genet. Dev. **22**, 191 (2012).
10. Y. Miki et al., Cancer Res. **52**, 643 (1992).
11. R. C. Iskow et al., Cell **141**, 1253 (2010).
12. P. J. Hastings, G. Ira, J. R. Lupski, PLoS Genet. **5**, e1000327 (2009).
13. CRA00R was excluded from this assessment because the event frequency in this tumor was underestimated as a result of a data quality issue in the matched normal sample (see materials and methods).
14. G. Poulogiannis et al., Proc. Natl. Acad. Sci. U.S.A. **107**, 15145 (2010).
15. Z. Jin et al., Oncogene **26**, 6332 (2007).
16. M. L. Slovak et al., Clin. Cancer Res. **17**, 3443 (2011).
17. R. E. Dickinson, K. S. Fegan, X. Ren, S. G. Hillier, W. C. Duncan, PLoS One **6**, e27792 (2011).
18. H. Izumi et al., Hum. Mol. Genet. **14**, 997 (2005).
19. R. Beroukhim et al., Proc. Natl. Acad. Sci. U.S.A. **104**, 20007 (2007).
20. H. Zheng et al., Cancer Cell **17**, 497 (2010).
21. J. S. Han, S. T. Szak, J. D. Boeke, Nature **429**, 268 (2004).
22. M. L. Lin et al., Cancer Sci. **100**, 1443 (2009).
23. C. R. Beck et al., Cell **141**, 1159 (2010).
24. A. D. Ewing, H. H. Kazazian Jr., Genome Res. **20**, 1262 (2010).
25. A. D. Ewing, H. H. Kazazian Jr., Genome Res. **21**, 985 (2011).

Dense Chromatin Activates Polycomb Repressive Complex 2 to Regulate H3 Lysine 27 Methylation

Wen Yuan,[1,2]* Tong Wu,[1,2]* Hang Fu,[1,2]* Chao Dai,[3] Hui Wu,[4,2] Nan Liu,[5,2] Xiang Li,[4,2] Mo Xu,[4,2] Zhuqiang Zhang,[2] Tianhui Niu,[1,2] Zhifu Han,[2] Jijie Chai,[2,6] Xianghong Jasmine Zhou,[3] Shaorong Gao,[2]† Bing Zhu[2]†

Polycomb repressive complex 2 (PRC2)—mediated histone H3 lysine 27 (H3K27) methylation is vital for Polycomb gene silencing, a classic epigenetic phenomenon that maintains transcriptional silencing throughout cell divisions. We report that PRC2 activity is regulated by the density of its substrate nucleosome arrays. Neighboring nucleosomes activate the PRC2 complex with a fragment of their H3 histones (Ala^{31} to Arg^{42}). We also identified mutations on PRC2 subunit Su(z)12, which impair its binding and response to the activating peptide and its ability in establishing H3K27 trimethylation levels in vivo. In mouse embryonic stem cells, local chromatin compaction occurs before the formation of trimethylated H3K27 upon transcription cessation of the retinoic acid—regulated gene CYP26a1. We propose that PRC2 can sense the chromatin environment to exert its role in the maintenance of transcriptional states.

Polycomb repressive complex 2 (PRC2) is a histone methyltransferase specific to histone H3 Lys^{27} (H3K27) (1–4), which regulates Polycomb gene silencing and X chromosome inactivation (5–9). E(z)/Ezh2, the subunit of PRC2 that contains the SET histone methyltransferase domain, is inactive, and the presence of two other essential subunits [ESC/EED and Su(z)12] is required for enzyme activity (10). PRC2 can be allosterically activated by trimethylated H3K27 (H3K27me3) (11) via its binding to ESC/EED (11, 12). PRC2 has little activity on mononucleosomes but exhibits robust activity on dinucleosomes (13), suggesting that PRC2 activity might be regulated by the density of its substrate chromatin.

We assembled three types of oligonucleosome substrates differing in octamer/DNA ratio (Fig. 1A

and fig. S1). Reconstituted Drosophila PRC2 complex (fig. S2) exhibited robust activity on dense oligonucleosomes and had far less activity on dispersed oligonucleosomes, despite the presence of equal amounts of histones (Fig. 1B). The results suggest that PRC2 activity might be regulated by two factors: the density of the substrate nucleosome arrays and/or the DNA content. The free DNA used for nucleosome assembly was titrated into dense oligonucleosomes, which partially inhibited PRC2 activity. However, PRC2 activity on dispersed oligonucleosomes remained 10-fold lower than that on the dense oligonucleosomes supplemented with higher amounts of free DNA (Fig. 1B), suggesting that the density of the substrate nucleosome arrays is a contributing factor in the regulation of PRC2 activity.

To verify our findings, we assembled mono- and dinucleosomes with different linker DNA (Fig. 1C). The strong nucleosome-positioning sequence 601 (14) was used to ensure the position of the assembled nucleosomes (fig. S3). Mononucleosomes were poor substrates, dinucleosomes were much better substrates for PRC2 (Fig. 1D) (10, 13), and PRC2 displayed lower activity on dinucleosomes with longer linker DNA (Fig. 1D). Together, these results suggest that PRC2 activity is sensitive to the density of its substrate chromatin.

PRC2 displayed much greater activity when a neighboring nucleosome was present (Fig. 1), suggesting that some feature(s) of the neighboring nucleosomes might activate PRC2. Indeed, a fragment of histone H3 (amino acids 31 to 42) (fig. S4A) greatly stimulated PRC2 enzyme activity (Fig. 1E) but not other tested histone methyltransferases (Fig. 1F and fig. S4). Scrambled peptides with identical amino acid composition

[1]College of Biological Sciences, China Agricultural University, Beijing 100094, China. [2]National Institute of Biological Sciences, Beijing 102206, China. [3]Program in Molecular and Computational Biology, University of Southern California, Los Angeles, CA 90089, USA. [4]Peking Union Medical College and Chinese Academy of Medical Sciences, Beijing 100730, China. [5]Beijing Normal University, Beijing 100875, China. [6]Tsinghua University, Beijing 10084, China.

*These authors contributed equally to this work.
†To whom correspondence should be addressed. E-mail: zhubing@nibs.ac.cn (B.Z.); gaoshaorong@nibs.ac.cn (S.G.)

Landscape of Somatic Retrotransposition in Human Cancers

Eunjung Lee, Rebecca Iskow, Lixing Yang, Omer Gokcumen, Psalm Haseley, Lovelace J. Luquette, III, Jens G. Lohr, Christopher C. Harris, Li Ding, Richard K. Wilson, David A. Wheeler, Richard A. Gibbs, Raju Kucherlapati, Charles Lee, Peter V. Kharchenko, Peter J. Park, and The Cancer Genome Atlas Research Network

Movement in the Cancer Genome

Transposable elements are genetic sequences that can replicate and move within the genome. The factors that make an element mobile are unknown but are generally considered rare in mammals. Lee *et al.* (p. 967, published online 28 June) analyzed five cancer types occurring among several individuals and found that three types of epithelial tumors exhibited high rates of element movement relative to brain and blood cancers. Furthermore, these somatically acquired, tumor-specific elements targeted genes in colorectal cancer that, when disrupted, impact gene expression and thus may be a factor in the progression of the cancers.

View the article online
https://www.science.org/doi/10.1126/science.1222077
Permissions
https://www.science.org/help/reprints-and-permissions

Use of this article is subject to the Terms of service